Journal of Science Research and Reviews

PRINT ISSN: 1595-9074
E-ISSN: 1595-8329
DOI: https://doi.org/10.70882/josrar.2025.v2i6.133
Homepage: https://josrar.esrgngr.org

Original Research Article

A Density Functional Theory Study on Effect of Cations and Anions Co-Alloyed Cu_2ZnSnS_4 Kieserite on Structural and Formation energy as possible Photovoltaic Material

***[1]Masanawa, Aliyu A., [2]Shuaibu, Alhassan and [2]Aliyu, Muhammed M.**

[1]Applied Physics Department, Kaduna Polytechnic.
[2]Department of Physics, Kaduna State University, Kaduna PMB 2339, Kaduna, Nigeria.
*Corresponding Author's email: alinmasanawa@gmail.com

KEYWORDS

Kesterite,
Density Functional Theory,
Solar cell,
Chalcogenide,
Alloying.

CITATION

Masanawa, A. A., Shuaibu, A., & Aliyu, M. M. (2025). A Density Functional Theory Study on Effect of Cations and Anions Co-Alloyed Cu2ZnSnS4 Kieserite on Structural and Formation energy as possible Photovoltaic Material. *Journal of Science Research and Reviews*, 2(6), 16-20. https://doi.org/10.70882/josrar.2025.v2i6.133

ABSTRACT

Cu_2ZnSnS_4 (CZTS) has the potential to be applied as an earth-relatively abundant and non-toxic material in thin-film solar cells, based on its suitable electrical and optical properties. However, many challenges have prevented the achievable efficiencies from exceeding 12.6%, which is well below desirable efficiencies compared to other competing solar cell technologies. One of the problems with the development of Cu_2ZnSnS_4 solar cells is the number of defects leading to severe potential fluctuations. This research work investigates the effect of alloying CZTS with Silver (Ag) (Cation) and Selenium (Se) (Anion) theoretically using Density Functional Theory (DFT). The optimized lattice parameters were found to increase from 5.26 to 5.85 and 10.60 to 12.32 respectively due to the introduction of Ag and Se. The volume of the crystal unit cell increased from 162.747 3 to 219.472 3 respectively. The formation energy was found to be reduced from 0.663eV to 0.476eV. From the obtained results, it can be seen that the alloyed $Ag_2ZnSnSe_4$ compound has a low-range energy structure and its stable within a low temperature range. This result is expected to enhance the properties of kesterite due to the alloying.

INTRODUCTION

The technology of the future must also progress by coming up with sustainable solutions that utilize accessible and non-toxic natural resources, as well as easy manufacturing procedures. In this context, earth-abundant and low-toxic solar devices could be very essential (Le Donne *et al.,* 2019). Kesterite materials, which belong to the chalcogenide family, are among the most promising. $CuInGaSe_2$ is known as CIGS and is typically produced by vacuum techniques that are followed by sintering in a selenide atmosphere. This is why, even if CIGS have the potential to perform well, its cost is still too high (Ramanujam and Singh, 2017). By substituting one tin (Sn^{+4}) and one zinc (Zn^{+2}) for indium (In^{+3}) and gallium (Ga^{+3}), kesterite-based photovoltaics based on Cu_2ZnSnS_4 (CZTS), $Cu_2ZnSnSe_4$ (CZTSe), and $Cu_2ZnSn(S,Se)_4$ (CZTSSe) are emerging as the most viable option (Liu *et al.,* 2016). Although kesterite-based solar cells perform less well than CIGS, they are constructed of abundant and non-toxic materials (Paire *et al.,* 2014). Kesterite is a mineral found in nature where zinc and iron share lattice positions. Kesterite can be manufactured in the laboratory as a p-type semiconductor material, and it has recently gained increased interest as a means of cutting the cost of thin-film photovoltaic production and minimizing environmental effects (Ito, 2015). Kesterite has a high absorption coefficient, around $105\ cm^{-1}$, and a direct band interval in the range of 1.0 to 1.5 eV, which enables practical photon capture at layer thicknesses of a few microns (Mitzi *et al.,* 2011).

As a photo-absorber, kesterite shows a high absorption coefficient and an optimal direct bandgap (Chen *et al.,* 2009). Additionally, the energy band gap can be controlled to allow for total or partial component replacement. As a result of their less hazardous and abundant components, appropriate band levels, and high absorption coefficients, kesterite compounds are attractive prospects for solar cell applications. According to Katagiri *et al.* (1997), the first kesterite solar cell was constructed using vacuum techniques in 1997, achieving a conversion efficiency of 0.66 percent; the current record efficiency of 12.6 percent was achieved by CZTSSe in 2014 (Wang *et al.,* 2014). Solar cells based on kesterite are constructed of abundant and non-toxic materials. With ideal band gaps and high absorption coefficients. But they tend to show lower performance than CIGS. The long-standing challenge facing kesterite solar cells is the large V_{OC} deficit, reported unanimously by various literature, which is also a focus of other researches both theoretically within DFT and experimentally, and that is ultimately due to non-radiative electron-hole recombination (Gokmen *et al.,* 2014). The contributing factors to this voltage deficit can include the presence of small-gap, cation disorder (example Cu–Zn antisites), interfacial reactions (e.g. SnS formation at the back contact), and deep-level defects (e.g. SnZn), It has been proven that the above mentioned problems can be addressed fully either by doping or alloying. This is because alloying kesterite enables the tuning of the properties of the material for advanced device engineering.

MATERIALS AND METHODS

The calculations were performed on a supercell structure relative to the standard conventional unit cell compounds. Using first principle calculation by Quantum ESPRESSO simulation package code within DFT. Within the Perdew-Burke-Ernzerhof generalized gradient approximation (PBE-GGA) (Perdew *et al.,* 1996), a pseudopotential was utilized to approximate the exchange-correlation potential for both pure Cu_2ZnSnS_4 and alloyed $Ag_2ZnSnSe_4$ Kesterite. Smearing, more precisely the Maxfessel-Paxton smearing method, was used for integrals. The Monkhorst-Pack technique was used to integrate the Brillouin zone. (Monkhorst and Pack, 1976) with $10 \times 10 \times 1$ and $12\times12\times1$ k-points grids for the pure and alloyed compound respectively.

For alloying in the Copper atomic site, all the copper atoms in the cells were replaced with Ag as cation alloyed and all the sulphur atoms are replaced with Selenium as anion alloyed. The cell dimensions are constant throughout the calculations, however, the atomic locations are completely loosened for all calculations using Broyden-Fletcher-Golfarb-Shanno (B.F.G.S.) algorithms, until the forces acting on the atoms are less than 0.001 eV (Wei, 2021).

RESULTS AND DISCUSSION

Results of the Convergence Test

Before beginning any DFT calculations using any code, it is critical to set up and conduct a convergence test calculation. This is to enable and obtained a well converged total energy the parameter is needed to attain certain stability and well converged points. This is because numerical converged value gives an approximated solution. The results shown below illustrate the convergence tests for pure kesterite Cu_2ZnSnS_4 and alloyed $Ag_2ZnSnSe_4$ with respect to the plane wave kinetic energy cut-off and K-point mesh.

Convergence Test Result for energy cut-off and K-point mesh of pure kesterite Cu_2ZnSnS_4

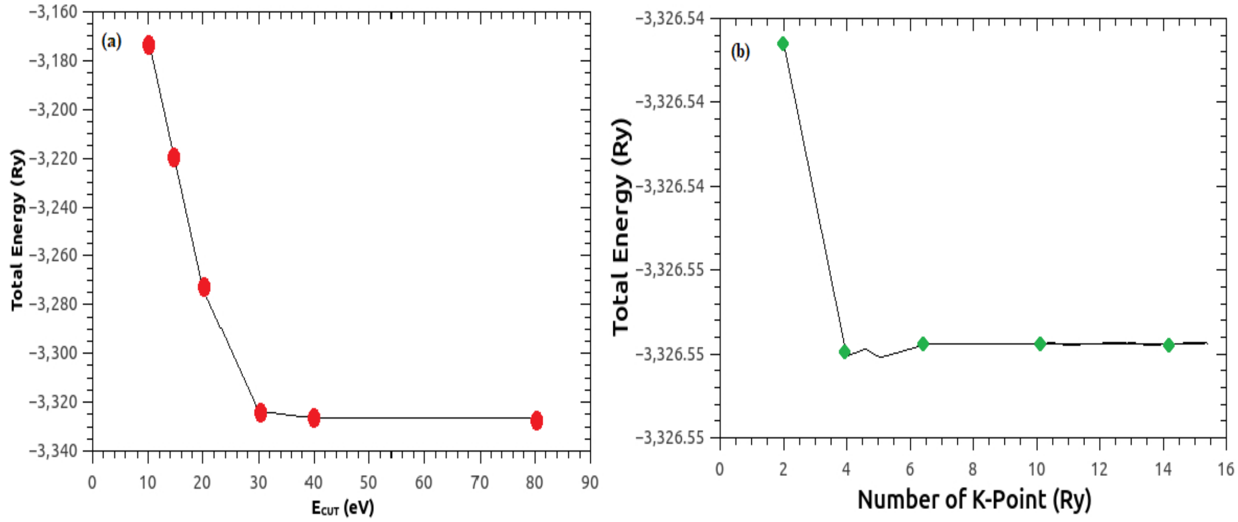

Figure 1: (a) The Convergence test of total energy in relation to the pure plane-wave energy cut-off (b) convergence of total energy in relation to pure kesterite k-point grids Cu_2ZnSnS_4

It can be seen from the graph of figure 1a and 1b shows the convergence test result of pure kesterite Cu_2ZnSnS_4 for the kinetic energy cut-off (eV) with respect to total energy E_{tot}. From Figure 1a it demonstrates that the total energy changes considerably with kinetic energy cut-off (eV) between 40-80eV where the energy becomes more stable with less or no effect on the total energy of the compound. The total energy remains constant as the kinetic energy cut-off is increased further, indicating a well-converged energy cut-off point. As a result, the plane wave set for the kinetic cut-off point was chosen to be 40 eV. However, as illustrated in Figure 1b, the total energy of pure kesterite Cu_2ZnSnS_4 varies significantly with k-point grids until reaching a well-converged value. The total energy increases from 4x4x1 to 14×14x1 k-points and becomes almost stable at 10×10×1. Therefore, 10×10×1 is considered as the most converged and optimized value for the k-points mesh grid for pure kesterite Cu_2ZnSnS_4.

Convergence Test Result for energy cut-off and K-point mesh of co-alloyed kesterite $Ag_2ZnSnSe_4$

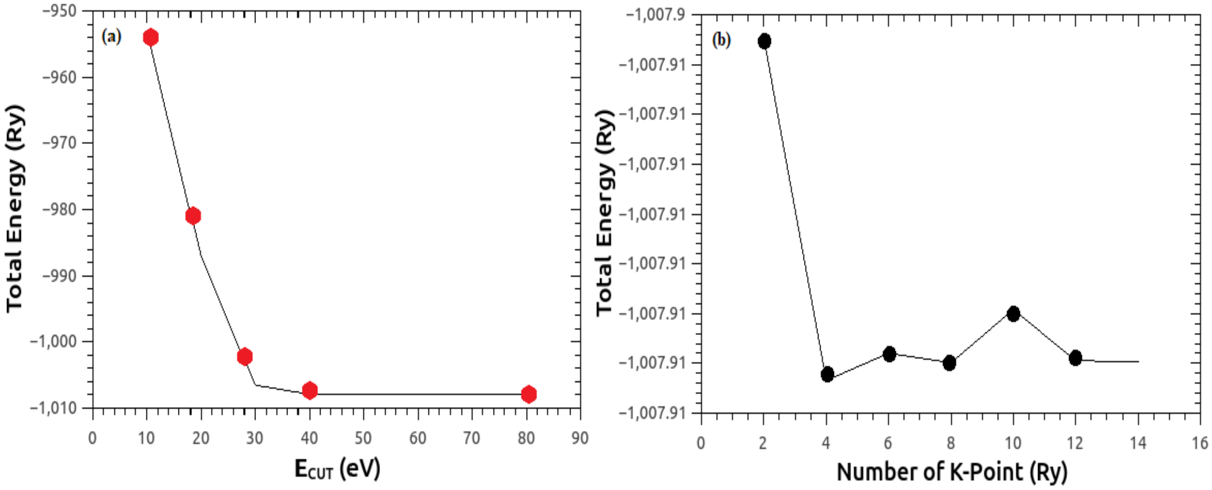

Figure 2: (a) The Convergence test of total energy in relation to the pure plane-wave energy cut-off (b) convergence of total energy in co-alloyed kesterite with regard to k-point grids $Ag_2ZnSnSe_4$

It can be seen from the graph of Figure 2a and 2b shows the convergence test result of alloyed kesterite $Ag_2ZnSnSe_4$ for the kinetic energy cut-off (eV) with respect to total energy E_{tot}. From Figure 2a, it demonstrates that the total energy changes considerably with kinetic energy cut-off (eV) between 40-80eV where the energy becomes more stable with less or no effect on the total energy of the compound. The total energy remains constant as the kinetic energy cut-off is increased further, indicating a well-converged energy cut-off point. As a result, the plane wave set for the kinetic cut-off point was chosen to be 40 eV.

However, Figure 2b illustrates the fluctuations in total energy with respect to k-point grids for alloyed kesterite $Ag_2ZnSnSe_4$, it can be observed from the figure the total energy changes considerably with k-point mesh until at a certain point showing a well converged value. The total energy increases from 4×4×1 to 14×14×1 k-points and becomes almost stable at 12×12×1. Therefore, 12×12×1 is considered as the most converged and optimized value for the k-points mesh grid for alloyed kesterite $Ag_2ZnSnSe_4$.

Structural Stability

Figure 3 shows the optimized tetragonal structure of both pure and alloyed compounds, the crystal consisted of 16 ions with four (4) atoms of copper (Cu), two atoms (2) of Zinc (Zn), two (2) atoms of tin (Sn) and eight (8) atoms of Sulphur (S) forms the initial compound Cu_2ZnSnS_4 Figure 3(a). In the model, all the 4 atoms of Cu and 8 atoms of S are replaced with silver Ag for cation alloying and Selenide Se for anion alloying respectively. The optimized lattice parameters "a" and "c" increase from 5.26 Å to 5.85 Å and 10.60 to 12.32 Å respectively due to the introduction of Ag and Se. The volume of the crystal unit cell increased from 162.747 $Å^3$ to 219.472 $Å^3$ respectively see Table 1. This increase is expected due to the larger size of the silver (Ag) and selenium (Se) atoms compared to that of Cu and S atoms. The findings are consistent with some theoretical predictions (Chen *et al.,* 2011; Gezgin *et al.,* 2019). By comparing the calculated formation energy Ef of the pure and alloyed compounds, the stability of each was inferred (See table 1). Although pure Cu_2ZnSnS_4 is known as lowest-energy structure, the obtained results -0.663eV confirmed that which are agreements with many reported (Ananthoju *et al.,* 2016). Similarly, the formation energy of the alloyed compound is obtained as -0.476eV which is also within the range of lowest-energy structure confirming the stability of the model compound $Ag_2ZnSnSe_4$.

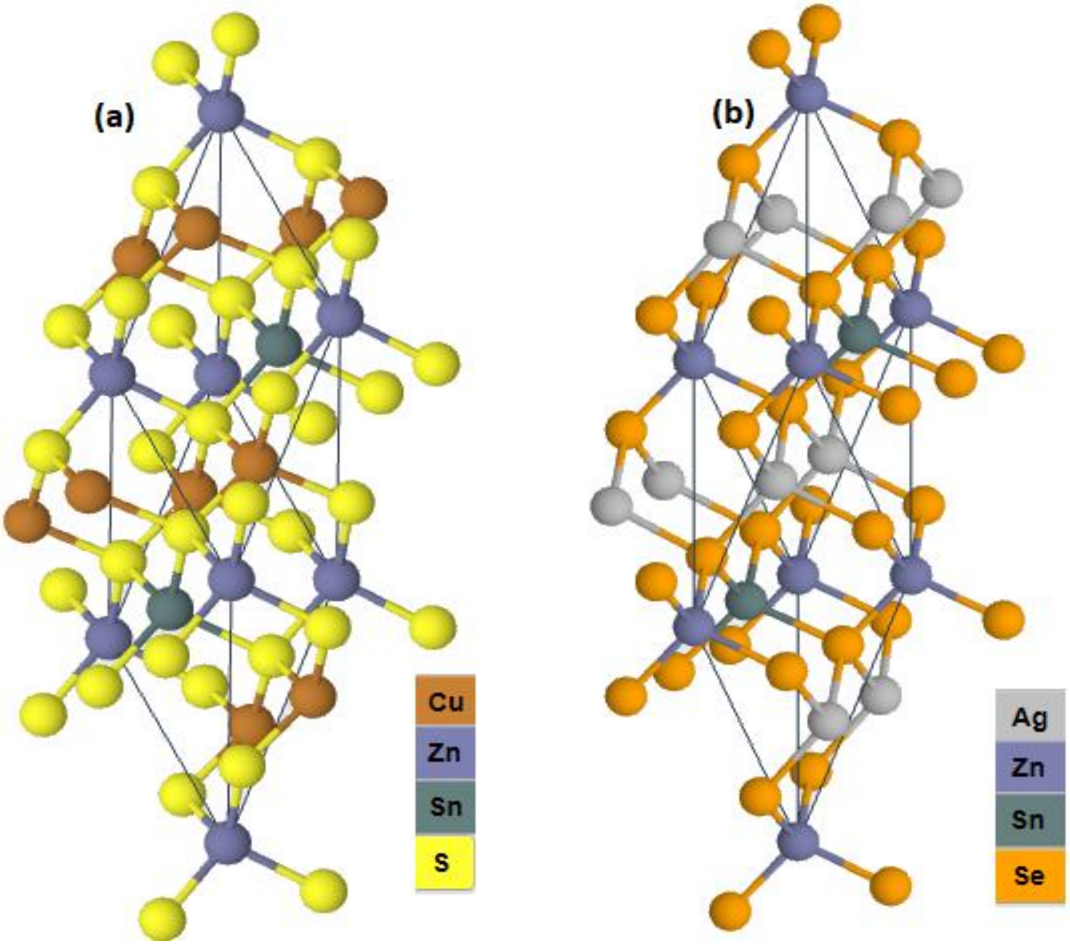

Figure 3: Optimized structure of (a) pure kesterite Cu_2ZnSnS_4 and (b) alloyed $Ag_2ZnSnSe_4$

Table 1: Calculated crystal parameters and formation energy E_f

Material	Crystal parameters	E_f (eV)
Cu_2ZnSnS_4	$a = 5.26Å, c = 10.60Å$	-0.663
	$a = 5.46\ Å, c = 10.90Å$ *	-0.705*
$Ag_2ZnSnSe_4$	$a = 5.85\ Å, c = 12.32Å$	-0.476
	$a = 5.91\ Å, c = 12.53Å$**	-0.585**

*Ananthoju *et al.,* (2016) ** Gershon *et al.,* (2017)

CONCLUSION

We have seen that by using first-principles methods, an alloyed compound of CZTS has been successfully modeled. The optimized lattice parameter, the volume of the crystal unit cell and the formation energy of both the pure and alloyed compounds were calculated respectively. From the obtained results it can be seen that the alloyed $Ag_2ZnSnSe_4$ compound is a low-range energy structure and stable within a low temperature range compared to the pure compound.

REFERENCES

Ananthoju, B., Mohapatra, J., Jangid, M. K., Bahadur, D., Medhekar, N. V., and Aslam, M. (2016). Cation/anion substitution in Cu_2ZnSnS_4 for improved photovoltaic performance. Scientific reports, vol 6(1), page 1-11.

Chen, S., Gong, X. G., Walsh, A., and Wei, S. H. (2011). Structural, electronic, and defect properties of $Cu_2ZnSn(S, Se)_4$ alloys. *MRS Online Proceedings Library (OPL)*, *1370*.

Chen, S., Gong, X., Walsh, A. and Wei, S. (2009). Crystal and electronic band structure of Cu_2ZnSnX_4 (x=S,Se) photovoltaic absorbers: First-principles in-sights. *Applied Physics Letter*. vol. 94, page 235.

Gershon, T., Sardashti, K., Lee, Y. S., Gunawan, O., Singh, S., Bishop, D., and Haight, R. (2017). Compositional effects in $Ag_2ZnSnSe_4$ thin films and photovoltaic devices. *Acta Materialia*. Vol. *126*, pages 383-388.

Gezgin, S. Y., Houimi, A., and Kılıç, H. Ş. (2019). Production and photovoltaic characterization of n-Si/p-CZTS heterojunction solar cells based on a CZTS ultrathin active layers. *Optik*, vol. *199*, page 163370.

Gokmen, T., Gunawan, O. and Mitzi, D.B. (2014). Semi-Empirical Device Model for $Cu_2ZnSn(S,Se)_4$ Solar Cells. *Applied Physics Letters*. Vol 105(3): p. 033903

Ito, K. (2015). Copper zinc tin sulphide-based thin film solar cells. Electronic Materials. Page 253. John Wiley & Sons, Ltd.

Katagiri, H., Sasaguchi, N., Hando, S., Hoshino, S., and Ohashi, J. (1997). Preparation and evaluation of Cu_2ZnSnS_4 thin films by sulfurization of EB evaporated precursors. *Solar Energy Materials and Solar Cells*. Vol. 49(1- 4): 407-414.

Le Donne, A., Trifiletti, V., and Binetti, S. (2019). New Earth-Abundant Thin Film Solar Cells Based on Chalcogenides. *Frontier Chemistry*. Vol. 7: page 297.

Liu, X., Feng, Y., Cui, H., Liu, F., Hao, X. (2016). The current status and future prospects of kesterite solar cells: a brief review. *Progress in Photovoltaics Research and Applications*. Vol. 24(6): Page 879-898.

Mitzi, D.B., Gunawan, O., Todorov, T.K., Wang, K., Guha, S. (2011). The path towards a high-performance solution-processed kesterite solar cell. *Solar Energy Materials and Solar Cells*. vol. 95(6): page 1421-1436.

Monkhorst, J.H., and Pack, J.D. (1976). Special Points for Brillouin-zone Integration. *Physical Review B*. vol. 13 page 5188.

Paire, M., Delbos, S., Vidal, J., Naghavi, N., Guillemoles, J.F. (2014). Chalcogenide Thin-Film Solar Cells. In Solar Cell Materials pp 145-215, John Wiley & Sons, Ltd.

Perdew, J.P., Kieron, B., and Matthias, E. (1996). Generalized Gradient Approximation Made Simple. *Physical Review Letters*. Vol. 77 page. 3865.

Ramkumar, S. P., Gillet, Y., Miglio, A., van Setten, M. J., Gonze, X. and Rignanese, G.-M. (2016). First-principles Investigation of the Structural, Dynamical, and Dielectric Properties of Kesterite, Stannite, and PMCA Phases of Cu_2ZnSnS_4. *Physical Review B*, vol. 94, p. 224302.

Wang, W., Winkler, M.T., Gunawan, O., Gokmen, T., Todorov, T.K. (2014). Device Characteristics of CZTSSe Thin-Film Solar Cells with 12.6% Efficiency. *Advanced Energy Materials*. Vol. 4(7): page 1301465.